Tracking halo coronal mass ejections from 0–1 AU and space weather forecasting using the Solar Mass Ejection Imager (SMEI)

T. A. Howard,[1,2] D. F. Webb,[3] S. J. Tappin,[1] D. R. Mizuno,[3] and J. C. Johnston[4]

Received 3 August 2005; revised 4 January 2006; accepted 26 January 2006; published 29 April 2006.

[1] The Solar Mass Ejection Imager (SMEI) has been tracking coronal mass ejections (CMEs) from the Sun to the Earth and beyond since it came online in February 2003. This paper presents some results from the first 19 months of data from SMEI, when over 140 transients of many kinds were observed in SMEI's all-sky cameras. We focus specifically on 20 earthward directed transients, and compare distance-time plots obtained from the SMEI transients with those observed in halo CMEs by Large-Angle Spectrometric Coronograph (LASCO) aboard Solar and Heliospheric Observatory (SOHO), and the arrival time of the shock observed by ACE at 0.99 AU. The geometry of one particular transient is compared using both LASCO and SMEI images in a first attempt to investigate geometry evolution as the transient propagates through the interplanetary medium. For some events, the halo CME, SMEI transient, and shock at 0.99 AU do not match, suggesting that some transients may not correspond to a halo CME. Finally, an evaluation of the potential of SMEI to be used as a predictor of space weather is presented, by comparing the transients observed in SMEI with the 22 geomagnetic storms which occurred during this timeframe. A transient was observed in 14 cases, and distance-time profiles would have allowed a prediction of the arrival time at ACE within 2 hours of its actual arrival for three events, and within 10 hours for eight events. Of these eight events, seven were detected by SMEI more than 1 day before the transient's arrival at the Earth.

Citation: Howard, T. A., D. F. Webb, S. J. Tappin, D. R. Mizuno, and J. C. Johnston (2006), Tracking halo coronal mass ejections from 0–1 AU and space weather forecasting using the Solar Mass Ejection Imager (SMEI), *J. Geophys. Res.*, *111*, A04105, doi:10.1029/2005JA011349.

1. Introduction

[2] Coronal mass ejections (CMEs) are generally believed to be responsible for major geomagnetic disturbances at the Earth. These so-called geomagnetic storms are initiated when an interplanetary transient impacts with the magnetosphere, causing an enhancement of the Earth's ring current and aurora [e.g., *Dungey*, 1961], and consequently a variety of other deleterious effects. Earthward directed CMEs appear in coronagraphs as expanding halos around the occulting disk, and are hence termed halo CMEs [*Howard et al.*, 1982]. These evolve into interplanetary transients and are detected near the Earth as shocks and ejecta. A partial halo is generally regarded as a CME which has a projected width $\geq 120^\circ$ [*Yashiro et al.*, 2004]. Halo and partial halo CMEs observed in LASCO are henceforth referred to as HCMEs. The connection between earthward HCMEs and interplanetary shocks [*Gonzalez and Tsurutani*, 1987; *Gosling et al.*, 1990, 1991; *Echer et al.*, 2004] and with geomagnetic storms [*Sheeley et al.*, 1985; *Fox et al.*, 1998; *Webb et al.*, 2000, and references therein] has been well established.

[3] Although there are several instruments currently in operation which observe regions close to the Sun and the Earth, there is a very large spatial gap for these instruments from $\sim$0.15–0.99 AU. Some attempts have been made to observe transients within this gap using interplanetary scintillation (IPS) [*Hewish et al.*, 1964, 1985; *Readhead et al.*, 1978]. This technique traditionally detects fluctuations in meter-wave radio signals across the sky, caused by density irregularities in the solar wind. This technique has been successful in the past at tracking some large interplanetary transients [*Gapper et al.*, 1982; *Hewish et al.*, 1985]. Tomographic methods have also been employed with IPS data to estimate the three-dimensional structure of transients [e.g., *Jackson et al.*, 1997], along with data from the Helios spacecraft [*Jackson and Hick*, 2002; *Jackson et al.*, 2004b, and references therein].

[1]School of Physics and Astronomy, University of Birmingham, Edgbaston, UK.
[2]Now at Department of Physics, Montana State University, Bozeman, Montana, USA.
[3]ISR, Boston College, Chestnut Hill, Massachusetts, USA.
[4]Space Weather Center of Excellence, Air Force Research Laboratory, Hanscom AFB, Massachusetts, USA.

0148-0227/06/2005JA011349$09.00

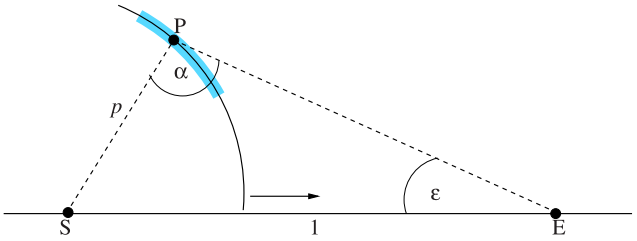

Figure 1. Diagram of the geometry for the Point P approximation. S and E are the locations of the Sun and Earth, respectively, and the transient is represented by an arc with its center at S. P is the location of the point on the transient at which the SMEI measurement has been made. Let ∠SEP = ϵ, the elongation angle and ∠SPE = α. Also, let p be the distance from the Sun to point P (SP). If we assume the transient is spherical, then PE becomes a tangent and $\alpha = \pi/2$.

[4] The Solar Mass Ejection Imager (SMEI) [*Eyles et al.*, 2003; *Jackson et al.*, 2004b] was launched aboard the Coriolis spacecraft on 6 January 2003, and consists of three CCD cameras which observe almost the entire sky in white light on each 102-min orbit. It was conceived as an all-sky coronagraph [*Jackson et al.*, 1989] and is designed to monitor interplanetary disturbances propagating from the Sun. The instrument may be regarded as a successor to the zodiacal-light photometers of the twin Helios spacecraft [*Leinert et al.*, 1975]. *Tappin et al.* [2004] reported the first SMEI observations of a large disturbance observed at the Sun as a HCME by LASCO on 28 May 2003, which caused a large geomagnetic storm on 30 May. They identified an interplanetary transient with SMEI which propagated through the sky between 0.2 and 1 AU during 29 May. Distance-time plots of the transient obtained from the SMEI images matched well with those produced for the HCME observed in LASCO, and permitted a prediction of the arrival of the shock at ACE within 2 hours of its actual arrival. IPS techniques have also been used on SMEI data to model the three-dimensional structure of some interplanetary transients [*Tokmuraru et al.*, 2004; *Jackson et al.*, 2004a].

[5] This paper presents results from a study using SMEI data to track earthward interplanetary transients from the Sun to the Earth. We compare HCMEs observed at the Sun with transients observed between 0 and 1 AU by SMEI and consider their influence on the arrival of the associated shock near 1 AU. Of particular interest are those events which caused geomagnetic storms, and CME geometry and speed evolution are also considered. Finally, an evaluation of the potential of SMEI, or a SMEI-like instrument for space weather forecasting is given, using distance-time (d-t) profiles to estimate the arrival of the transient at ACE and comparing it with the actual arrival time of the measured forward shock.

2. Data and Analysis

[6] The SMEI instrument provided the basis for the present study. Data for the first 19 months of SMEI observations (10 February 2003 until 31 August 2004) were used. Distance-time profiles were measured from all-sky Aitoff images, with the leading structure measured in each case. Figure 1 of *Tappin et al.* [2004] provides an example of a sequence of SMEI Aitoff images with an interplanetary transient.

[7] Owing to the nature of the coordinate system of the SMEI images, distances are given in units of elongation angle ϵ, which is the angle between the Sun-Earth line and a line from the Earth (E) to the measured point (P) on the transient. Let ∠SPE be α and p be the distance from the Sun to P (SP) in AU, as shown in Figure 1. Using this geometry,

$$\frac{p}{\mathrm{SE}} = \frac{\sin\epsilon}{\sin\alpha}. \tag{1}$$

If we assume the transient is earthward and the segment observed by SMEI approximates a spherical shape with the Sun at its center, then EP becomes a tangent to the sphere, (i.e., $\alpha = \pi/2$), and in units of AU, SE = 1. Therefore equation (1) becomes

$$p = \sin\epsilon. \tag{2}$$

This is known as the Point P approximation and allows a simplified, convenient conversion from elongation angle to distance in AU. This is generally an oversimplification, and the Point P approximation can be regarded as a lower limit estimate of the distance of the SMEI transient from the Sun. The Point P technique is used to estimate transient distance from the Sun in the present study.

[8] Coronagraph data were obtained from the Large-Angle Spectroscopic Coronagraph (LASCO) [*Brueckner et al.*, 1995] aboard the Solar and Heliospheric Observatory (SOHO). This instrument views the solar corona in white light with two coronagraphs: C2 (2.0–6.0 $R_\odot$) and C3 (3.7–30 $R_\odot$). Earthward transients were identified as HCMEs and d-t profiles were produced by measuring the leading structure of the brightest part of the HCME. Identification and some measurements were also obtained from the NRL CME list [*St. Cyr et al.*, 2000], available online at http://lasco-www.nrl.navy.mil/cmelist.html, and the CDAW Data Center CME catalog [*Yashiro et al.*, 2004], available at http://cdaw.gsfc.nasa.gov/CME_list/.

[9] Interplanetary shock data were provided by the MAG [*Smith et al.*, 1998] and the Solar Wind Electron Proton Alpha Monitor (SWEPAM) [*McComas et al.*, 1998] instruments aboard the ACE spacecraft. Both SOHO and ACE orbit the Sun at L1 (0.99 AU). An event was identified as an interplanetary shock if there was a unique, sudden (<3 min) significant increase in interplanetary magnetic field strength (B_{IMF}), density and solar wind speed across the same time range. The magnitude of the increase should exceed background fluctuations by at least a factor of 3.

Table 1. Definition of Storm Rating

Storm Rating	A_p	Dst
Small	~30 to 60	~−80 to −60
Medium	~60 to 80	~−150 to −80
Large	≥80	≤−150

Table 2. Possible Candidates for Earthward Transients From SMEI Observations[a]

Event Number	Date	DOY	Time UT	Direction	Reference
			2003		
1	17 Feb	048	1254	WNW	
2	19 March	078	1901	NNW	
3	6 April	096	1720 ×2	NW, WNW	
4	26 April	115	0502	NW	
5	28, 30 May	148, 150	1654, 1819	N	*Tappin et al.* [2004]
6	14 June	165	1036 ×2	NW	
7	17 Aug	229	0504	NE	
8	23, 24 Oct	296, 297	1138 ×2, 0434 ×4	S, NW	
9	27, 28 Oct	300, 301	0649, 1304 ×2	W, SE, WNW	*Jackson et al.* [2006]
10	2 Nov	306	2154 ×2	NW, W	
11	14 Nov	318	0511	SE	
12	19 Nov	323	0548 ×2	SSE	
			2004		
13	6 Jan	006	0024	SE	
14	21 Jan	021	0349	SE	
15	22 Jan	022	0331	SE	
16	31 March	091	1000	NNW	
17	10 May	131	0639	NNE	
18	15 July	197	1928	NW	
19	20, 21 July	202, 203	2129, 1602 ×2	WNW, NW	
20	29 July	211	0339	SW	

[a]The date, day of year (DOY), first observation time of the transient observed in SMEI, and the region of the sky in which the transient was observed is given. Those events labeled with a ×2 or ×4 indicate those for which more than one transient was identified in SMEI.

[10] Space weather data were obtained from the A_p (a daily derivation of the 3-hourly K_p index [*Bartels et al.*, 1939]) and Dst [*Sugiura*, 1964] indices from the Solar Geophysical Database. The magnitude of the storm was defined using both indices in accordance with *Howard and Tappin* [2005], as indicated in Table 1.

[11] The converted d-t profiles were fitted with a first-order least squares approximation (trendline) which was extended across the 0–1 AU range. This allowed an approximation of the "onset" of the transient at the Sun and its arrival at 1 AU. ACE shock and HCME combinations, provided by *Howard and Tappin* [2005], were compared with transients observed in SMEI. Time intervals where SMEI events occurred around the time of a shock-HCME combination were flagged as events for further analysis. In some cases, there was more than one SMEI transient in a single event. Using these selection criteria, we identified 20 events. These are listed in Table 2.

3. Results

3.1. A Likely Candidate

[12] Figures 2 and 3 show the event which first appeared as a slow arc to the southeast in SMEI data on 22 January 2004 at 0331 UT (event 15 in Table 2). Figures 2 and 3a show the LASCO C3 and SMEI images of the transient, and Figure 3b illustrates the geometry of each transient, with a position angle (PA)-distance plot of a sequence of images from both LASCO and SMEI. Finally, Figure 3c shows the d-t plot of the SMEI event, the associated HCME (which first appeared in the LASCO C2 coronagraph at 0454 UT on 21 January) and the time of arrival at ACE (1420 UT on 23 January). The curve representing a constant deceleration from the Sun to L1 [*Howard and Tappin*, 2005] is also shown. This event is believed to have been responsible for a medium storm (A_p = 64, Dst = −149), which began on 22 January. If we extend the least squares linear fit to the SMEI d-t data to cover the entire range of 0–1 AU, then we may estimate the time at which we expect the transient to leave the Sun and arrive at ACE. These times are 0705 UT on 21 January at the Sun and 1039 UT on 23 January at

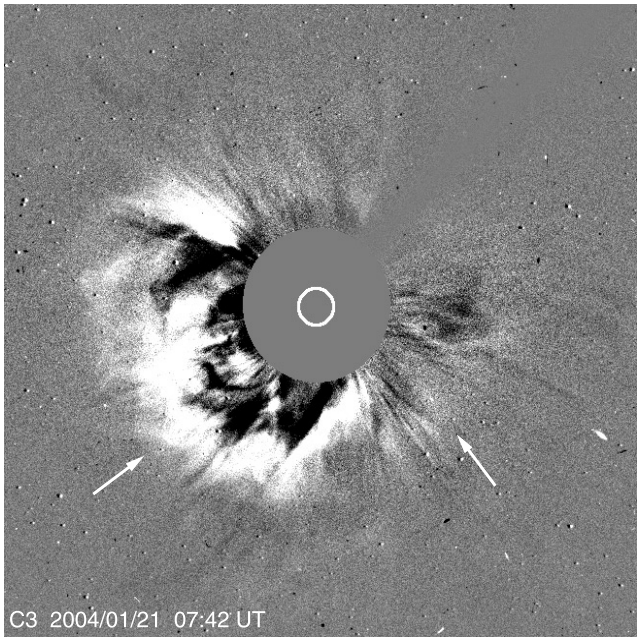

Figure 2. LASCO C3 image of the Halo CME on 0742 UT on 21 January 2004. There are two structures in this image, with the brighter element in the southeast quadrant and the fainter halo surrounding.

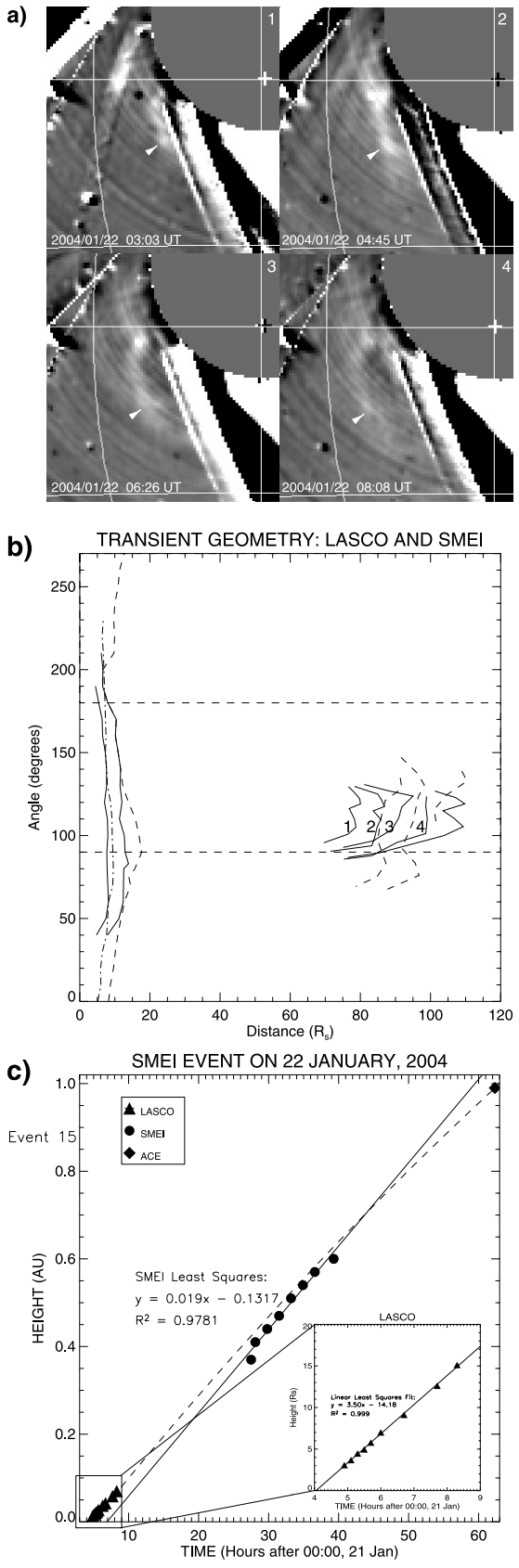

Figure 3. (a) SMEI image sequence of the transient shown in Figure 2 in the SE quadrant. The plus sign in each panel represents the location of the Sun. (b) Plot of position angle (PA) versus distance of the transients observed in the C3 and SMEI. The solid curves represent the geometry of the bright feature in the SW region of LASCO/SMEI, while the dashed curve represents the dimmer halo geometry. Times of each curve are 0618 and 0742 UT on 21 January 2004 (C3), and 0303, 0445, 0626, 0808, and 0949 UT for the bright feature and 0445, 0626, and 0808 UT for the halo on 22 January 2004 (SMEI). (c) Distance-time plot of the transient. Data are shown for LASCO and SMEI, and the time of arrival of the associated shock at ACE is indicated. Also shown are the curve for constant deceleration for this event [*Howard and Tappin*, 2005] and the linear trend for the SMEI d-t plot. The latter is extended to cover the full range from 0 to 1 AU. The LASCO d-t data are enlarged in the bottom right of the plot.

ACE. We believe the events observed in LASCO, SMEI, ACE and at the Earth to be due to the same transient, and our estimate of the arrival time of the transient at ACE would have been only 3 hours, 41 min early.

[13] Figure 3b shows the geometry of the leading structure for successive images obtained from LASCO and SMEI. The numbers correspond to the labels on each of the images from Figure 3a. The solid curve is believed to be connected with the bright feature of the transient, while the dashed curve is believed to be connected with the fainter "halo" component. The SMEI measurement is cut off toward the west by the shutter at $\sim$130° PA, and hence only a small part of the transient was observed in SMEI when compared with LASCO. However, some geometrical structure appears to be maintained, and some features enhanced. For example, the SMEI images show a clear trough in the geometrical structure of the bright feature at PA $\sim$ 115°, which probably matches with the slight trough in one LASCO images at PA $\sim$ 120°. The peaks are less easily defined, but the general geometrical structure appears to be more pronounced. The peak in the halo component of the transient appears to be moving with angle, from $\sim$90° at 0742 UT on 21 January to $\sim$82° at 0626 UT and $\sim$75° at 0808 UT on 22 January. This may be due to projection effects.

3.2. Summary

[14] A summary of d-t plots for each of the remaining 17 events (ignoring events 6 and 10, which are discussed by *Tappin et al.* [2004] and *Jackson et al.* [2006]) are shown in Figures 4 and 5. Note that in several cases there was more than one SMEI transient and HCME which occurred in the same time period. The SMEI events which were deemed to be the most relevant to the HCME-shock pair are labeled with solid circles with the other events as open circles. In some cases (such as events 11 and 18 on 14 November 2003 and 15 July 2004 respectively), the SMEI points are lower (i.e., have smaller distances) than are expected to fit the trend between the LASCO profile and shock time. This may be due to an inaccurate estimate of the Point P approximation, which provides a lower limit to the distance values.

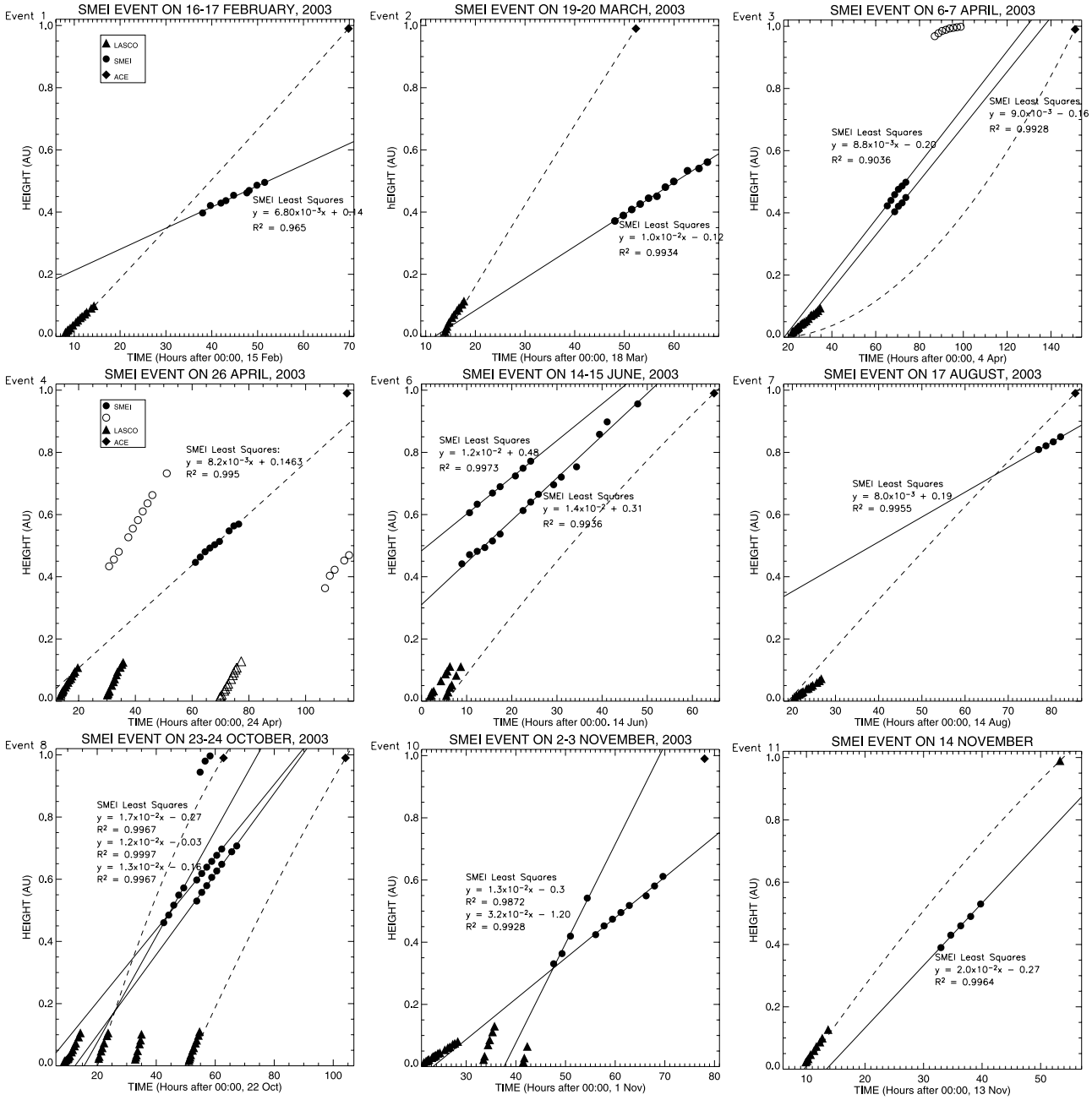

Figure 4. Distance-time profiles for nine of the remaining events from 2003. Shown are LASCO and SMEI d-t plots for every HCME and transient observed during the time range of each event, along with the time of the forward shock in ACE and the estimated constant deceleration curve. Also shown are the least squares linear fit to the SMEI data. Events 5 and 9 are discussed by *Tappin et al.* [2004] and *Jackson et al.* [2004a], respectively, and are hence not included in this figure.

3.3. Effectiveness as a Space Weather Tool

[15] During the time period covered by the present study, there were 22 geomagnetic storms which met the criteria described in Table 1. Of those, 14 (or 64%) were associated with an event observed by SMEI. For each of these events the arrival time of the transient at L1 was estimated using the SMEI d-t plots and compared with the actual arrival time at ACE. This is shown in Table 3. We identified three events for which projections of the d-t trendline predicted the arrival at ACE within 2 hours of their actual arrival, and eight (including the aforementioned three) events within 10 hours. Those six events with a predicted arrival time greater than 10 hours different from the actual arrival may not correspond to events observed by LASCO and/or ACE.

[16] Also shown in Table 3 is the difference in time between the transient's first observation in SMEI data and its arrival at ACE. Ten of the events were first detected in SMEI more than a day before the shock arrived at ACE, and the shortest delay was just under 9 hours. Of the eight events for which the arrival time was predicted within

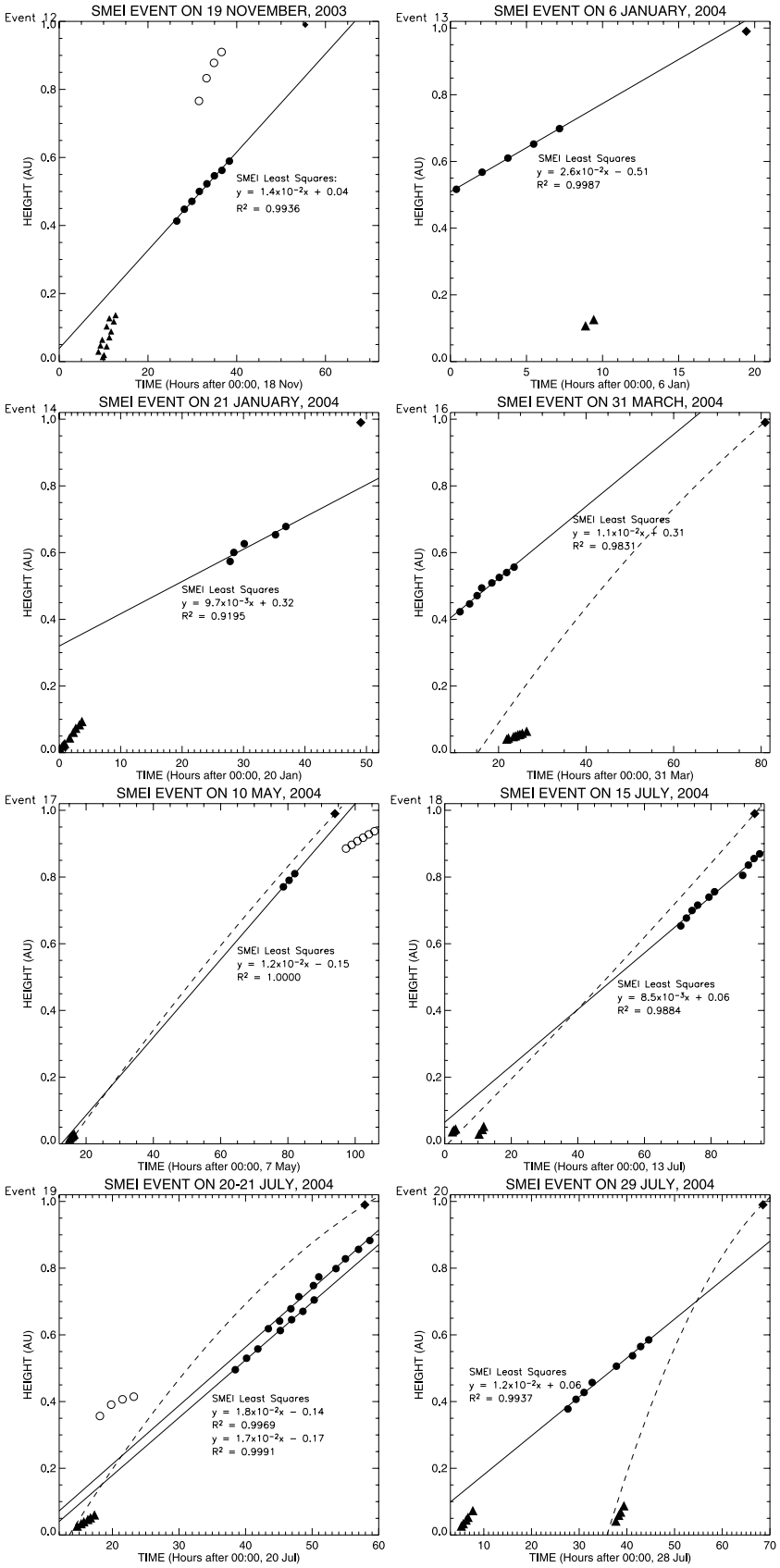

Figure 5. Distance-time profiles for one event in 2003 and seven of the remaining events from 2004. Details shown are identical to those in Figure 4.

Table 3. Effectiveness of SMEI as a Space Weather Tool[a]

Date	Time of Shock UT	Predicted Time of Shock Arrival UT	Difference	Difference from First Detection in SMEI	Storm Type	SSC UT
			2003			
29 March	0410	0553	0143 late	2d 14h 37m	small	no
29 May[b]	1830	2023	0153 late	1d 1h 36m	large	12–15
16 June[b]	1648	0200	14:48 early	2d 6h 12m	small	no
17 Aug[b]	1341	2743	1402 late	0d 8h 37m	large	15–18
24 Oct[b]	1449	2550	1101 late	1d 3h 11m	small	15–18
29 Oct[b]	0559	1207	0540 late	1d 23h 10m	large	6–9
	0627	2106	1439 late	0d 23h 3m		
04 Nov[b]	0600	0318 or 2642	0918 early or 2042 late	1d 5h 24m	medium	6–9
15 Nov[b]	0519	1456	0937 late	1d 0h 8m	small	6–9
19 Nov[b]	0727	1838	1111 late	0d 15h 29m	large	6–9
			2004			
06 Jan	1927	1813	0114 early	0d 19h 3m	small	18–21
22 Jan[b]	0105	2106	2001 late	0d 21h 16m	medium	0–3
23 Jan[b]	1420	1039	0341 early	1d 10h 49m	small	no
03 April[b]	0855	0846	2409 early	2d 22h 55m	medium	9–12
22 July[b]	0955	1624	0629 late	1d 12h 26m	medium	9–12

[a]Shown are the date, time of arrival of the forward shock measured by ACE, predicted time of shock arrival as estimated by the SMEI d-t plots, and the difference between the two. The time difference between the transient's first detection in SMEI and its arrival at ACE is shown as days (d), hours (h), and minutes (m). Also shown are the type of geomagnetic storm caused at the Earth and the UT times at which an associated SSC (if any) occurred.
[b]Events which were connected with a HCME at the Sun.

10 hours, seven were detected by SMEI more than 1 day before the shock's arrival.

[17] We have also performed two other studies of SMEI's utility in detecting and tracking those CMEs that subsequently cause major storms at Earth [see *Johnston et al.*, 2004]. Each study covered a 2-year period. First, we examined the sources of the most intense (peak Dst < -100 nT) geomagnetic storms during the period. There were 14 such storms and SMEI had suitable operations during 12 of them. During 10 of those 12 periods (83%), SMEI observed associated earthward directed transients. During all 12 storm periods, SMEI also observed the bright auroral light that was associated with the storm. The mean time difference between when SMEI first observed the transient and when its associated shock arrived at Earth was 18.6 hours. The mean difference between when SMEI first observed the transient and when the storm began was 29.25 hr. The second study included all moderate or greater storms (peak Dst < -60 nT) over a similar 2-year time period. For 85% (39 of 46) of these storms, SMEI detected a transient within 2 days prior to the onset of the storm.

[18] The above two studies investigated those events which were geoeffective, the former focused on events which produced large storms and the latter on events associated with moderate to weak storms. In the present study, to identify the time of arrival of the transient near 1 AU, we have focused only on those events which produced a shock detected by ACE. Thus a subset of these events are also included where appropriate in the data sets of the other two studies. The proportion of geoeffective transients observed by SMEI for the other two studies was ~20% higher than that of the transients in the present study. However, in all three studies, a large majority of the geoeffective transients were detected. Thus the main conclusion is that SMEI can detect the interplanetary transients causing most major geomagnetic storms from 10 hours to 2 days before storm onset, and can track the transients providing potential early warning of their arrival.

4. Discussion

[19] These results provide new information on the behavior of CMEs as they propagate through the interplanetary medium. In each case the transients appeared to propagate with a near-constant speed, implying that, at least for the cases in the present paper, any deceleration or acceleration process must occur when the transient is relatively close to the Sun (i.e., within ~0.3 AU). This has been discussed by *Reiner et al.* [2005] and *Tappin* [2006]. There is also potential to track the geometry of the transients as they evolve into the interplanetary medium.

[20] The polar orbit of the Coriolis spacecraft poses problems for clear detection and tracking of interplanetary transients as this orbit often takes the spacecraft through the magnetospheric cusp and polar cap, and also the South Atlantic Anomaly. Particles from these regions can saturate the cameras, making all-sky imaging difficult, and almost impossible during geomagnetic storms. It is therefore difficult to match the geometry of the interplanetary transients with those of the HCMEs. This means that identification of associated transients with the HCME/shock events has been achieved by matching the times of the events only, and so some connections may be purely coincidental. This may be the case for the six events which predicted the arrival of the shock by more than 10 hours (Table 3).

[21] Assuming that all of the transients observed in the present study were connected with the HCMEs and forward shocks, then SMEI identified 64% of them, 31% were detected over a day before they arrived, and 38% would have been predicted to arrive within 10 hours of their actual arrival at L1. We accept that while the "hit rate" for CME detection is relatively high the number of events for which we may make an accurate prediction is somewhat low.

However, for this small number of events, in terms of accuracy of arrival time this is better than any instrument in operation at present. Finally, these studies demonstrate the principal that, given adequate data latency, a SMEI-type instrument can detect the CMEs causing most major geomagnetic storms hours to days in advance, thus providing early warning of their arrival.

[22] **Acknowledgments.** SMEI was designed and constructed by a team of scientists and engineers from the U.S. Air Force Research Laboratory, the University of California at San Diego, Boston College, Boston University, and the University of Birmingham in the United Kingdom. SOHO is a project of international cooperation between ESA and NASA, and the SOHO/LASCO catalogs are maintained by NASA, Catholic University of America and the U.S. Naval Research Laboratory (NRL). They are made available courtesy of Goddard Space Flight Center and NRL. The Solar Geophysical Database is supported and maintained by NOAA and made available courtesy of the Solar-Terrestrial Physics Division. The work of D. F. Webb and D. R. Mizuno was supported in part by AF19628-00-C-0073.

[23] Shadia Rifai Habbal thanks Douglas A. Biesecker and Kenneth P. Dere for their assistance in evaluating this paper.

References

Bartels, J., N. H. Heck, and H. F. Johnston (1939), The 3-hour-range index measuring geomagnetic activity, *J. Geophys. Res.*, *44*, 411.

Brueckner, G. E., et al. (1995), The Large Angle Spectroscopic Coronagraph, *Sol. Phys.*, *162*, 357.

Dungey, J. W. (1961), Interplanetary magnetic field and the auroral zones, *Phys. Rev. Lett.*, *6*, 47.

Echer, E., M. V. Alves, and W. D. Gonzalez (2004), Geoeffectiveness of interplanetary shocks during solar minimum (1995–1996) and solar maximum (2000), *Sol. Phys.*, *221*, 361.

Eyles, C. J., G. M. Simnett, M. P. Cooke, B. V. Jackson, A. Buffington, N. R. Waltham, J. M. King, P. A. Anderson, and P. E. Holladay (2003), The solar mass ejection imager (SMEI), *Sol. Phys.*, *217*, 319.

Fox, N. J., M. Peredo, and B. J. Thompson (1998), Cradle to grave tracking of the January 6–11, 1997 Sun-Earth connection event, *Geophys. Res. Lett.*, *25*, 2461.

Gapper, G. R., A. Hewish, A. Purvis, and P. J. Duffet-Smith (1982), Observing interplanetary disturbances from the ground, *Nature*, *296*, 633.

Gonzalez, W. D., and B. T. Tsurutani (1987), Criteria of interplanetary parameters causing intense magnetic storms (Dst < −100 nT), *Planet. Space Sci.*, *35*, 1101.

Gosling, J. T., S. J. Bame, D. J. McComas, and J. L. Phillips (1990), Coronal mass ejections and large geomagnetic storms, *Geophys. Res. Lett.*, *17*, 901.

Gosling, J. T., D. J. McComas, J. L. Phillips, and S. J. Bame (1991), Geomagnetic activity associated with earth passage of interplanetary shock disturbances and coronal mass ejections, *J. Geophys. Res.*, *96*, 7831.

Hewish, A., P. F. Scott, and D. Wills (1964), Interplanetary scintillation of small diameter radio sources, *Nature*, *203*, 1214.

Hewish, A., S. J. Tappin, and G. R. Gapper (1985), The origin of strong interplanetary shocks, *Nature*, *314*, 137.

Howard, R. A., D. J. Michels, N. R. Sheeley Jr., and M. J. Koomen (1982), The observation of a coronal transient directed at Earth, *Astrophys. J.*, *263*, L101.

Howard, T. A., and S. J. Tappin (2005), Statistical survey of earthbound interplanetary shocks, associated coronal mass ejections and their space weather consequences, *Astron. Astrophys.*, *440*, 373.

Jackson, B. V., and P. P. Hick (2002), Corotation tomography of heliospheric features using global Thomson scattering data, *Sol. Phys.*, *211*, 344.

Jackson, B. V., H. S. Hudson, J. D. Nichols, and R. E. Gold (1989), in *Solar System Plasma Physics*, *Geophys. Monogr. Ser.*, vol. 54, edited by J. H. Waite Jr., J. L. Burch, and R. L. Moore, p. 291, AGU, Washington, D. C.

Jackson, B. V., P. L. Hick, M. Kojima, and A. Yokobe (1997), Heliospheric tomography using interplanetary scintillation observations, *Phys. Chem. Earth*, *22*, 425.

Jackson, B. V., A. Buffington, and P. P. Hick (2004a), Heliospheric photometric images and 3D reconstruction from the solar mass ejection imager (SMEI) data, *EOS Trans. AGU*, *85*(47), Fall Meet. Suppl., SH11A-02.

Jackson, B. V., et al. (2004b), The solar mass-ejection imager (SMEI) Mission, *Sol. Phys.*, *225*, 177.

Jackson, B. V., A. Buffington, P. P. Hick, X. Wang, and D. F. Webb (2006), Preliminary three-dimensional analysis of the heliospheric response to the 28 October 2003 CME using SMEI white-light observations, *J. Geophys. Res.*, doi:10.1029/2004JA010942, in press.

Johnston, J. C., J. B. Mozer, R. R. Radick, P. E. Holladay, T. A. Kuchar, D. R. Mizuno, and D. F. Webb (2004), Heliospheric imagers for tracking coronal mass ejections: Lessons learned from the Solar Mass Ejection Imager, *EOS Trans. AGU*, *85*(47), Fall Meet. Suppl., SH11A-05.

Leinert, C., H. Link, E. Pitz, N. Salm, and D. Knuppelberg (1975), The Helios zodiacal light experiment (E9), *Raumfahartforschung*, *19*, 264.

McComas, D. J., S. J. Blame, P. Barker, W. C. Feldman, J. L. Phillips, P. Riley, and J. W. Griffee (1998), Solar Wind Electron, Proton and Alpha Monitor (SWEPAM) for the advanced composition Explorer spacecraft, *Space Sci. Rev.*, *86*, 563.

Readhead, A. C. S., M. C. Kemp, and A. Hewish (1978), The spectrum of small-scale density fluctuations in the solar wind, *Mon. Not. R. Astron. Soc.*, *185*, 207.

Reiner, M. J., B. V. Jackson, D. F. Webb, D. R. Mizuno, M. L. Kaiser, and J. L. Bougeret (2005), CME kinematics deduced from white-light (SMEI) and radio (Wind/WAVES) observations, *J. Geophys. Res.*, *110*, A09S14, doi:10.1029/2004JA010943.

Sheeley, N. R., Jr., R. A. Howard, D. J. Michels, M. J. Koomen, R. Schwenn, K. H. Mulhauser, and H. Rosenbauer (1985), Coronal mass ejections and interplanetary shocks, *J. Geophys. Res.*, *90*, 163.

Smith, C. W., M. H. Acuna, L. F. Burlaga, J. L'Heureux, N. F. Ness, and J. Scheifele (1998), The ACE magnetic field experiment, *Space Sci. Rev.*, *86*, 613.

St. Cyr, O. C., et al. (2000), Properties of coronal mass ejections: SOHO LASCO observations from January 1996 to June 1998, *J. Geophys. Res.*, *105*, 18,169.

Sugiura, M. (1964), Hourly values of equatorial Dst for IGY, *Ann. Int. Geophys. Year*, *35*, 945.

Tappin, S. J. (2006), The deceleration of an interplanetary transient from the Sun to 5 AU, *Sol. Phys.*, *233*, 233.

Tappin, S. J., et al. (2004), Tracking a major interplanetary disturbance with SMEI, *Geophys. Res. Lett.*, *31*, L02802, doi:10.1029/2003GL018766.

Tokmuraru, M., M. Kojima, K. Fujiki, M. Yamashita, B. V. Jackson, and P. Hick (2004), Three-dimensional structure of compound interplanetary transients associated with 27–28 May 2003 coronal mass ejections, *Eos Trans. AGU*, *85*, Fall Meet. Suppl., SH11A-01.

Webb, D. F., E. W. Cliver, N. U. Crooker, O. C. St. Cyr, and B. J. Thompson (2000), Relationship of halo coronal mass ejections, magnetic clouds, and magnetic storms, *J. Geophys. Res.*, *105*, 7491.

Yashiro, S., N. Gopalswamy, G. Michalek, O. C. St. Cyr, S. P. Plunckett, and R. A. Howard (2004), A catalog of white light coronal mass ejections observed by the SOHO spacecraft, *J. Geophys. Res.*, *109*, A07105, doi:10.1029/2003JA010282.

T. A. Howard, Department of Physics, Montana State University, Bozeman, MT 59717, USA. (thoward@mithra.physics.montana.edu)

J. C. Johnston, Space Weather Center of Excellence, Air Force Research Laboratory, Hanscom AFB, MA 01731, USA.

D. R. Mizuno and D. F. Webb, ISR, Boston College, Chestnut Hill, MA 02467, USA.

S. J. Tappin, School of Physics and Astronomy, University of Birmingham, Edgbaston, B15 2TT, UK.